Chapter 10

Systematics of Renormalization

While computing radiative corrections in Chapters 6 and 7, we encountered three QED diagrams with ultraviolet divergences:

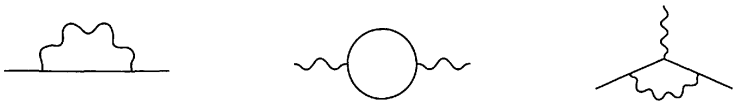

In each case we saw that the divergence could be regulated and canceled, yielding finite expressions for measurable quantities. In Chapter 8, we pointed out that such ultraviolet divergences occur commonly and, in fact, naturally in quantum field theory calculations. We sketched a physical interpretation of these divergences, with implications both in quantum field theory and in the statistical theory of phase transitions. In the next few chapters, we will convert this sketchy picture into a quantitative theory that allows precise calculations.

In this chapter, we begin this study by developing a classification of the ultraviolet divergences that can appear in a quantum field theory. Rather than stumbling across these divergences one by one and repairing them case by case, we now set out to determine once and for all which diagrams are divergent, and in which theories these divergences can be eliminated systematically. As examples we will consider both QED and scalar field theories.

10.1 Counting of Ultraviolet Divergences

In this section we will use elementary arguments to determine, tentatively, when a Feynman diagram contains an ultraviolet divergence. We begin by analyzing quantum electrodynamics.

First we introduce the following notation, to characterize a typical diagram in QED:

$$
\begin{aligned}
N_e &= \text{number of external electron lines;} \\
N_\gamma &= \text{number of external photon lines;} \\
P_e &= \text{number of electron propagators;} \\
P_\gamma &= \text{number of photon propagators;} \\
V &= \text{number of vertices;} \\
L &= \text{number of loops.}
\end{aligned}
$$

(This analysis applies to correlation functions as well as scattering amplitudes. In the former case, propagators that are connected to external points should be counted as external lines, not as propagators.)

The expression corresponding to a typical diagram looks like this:

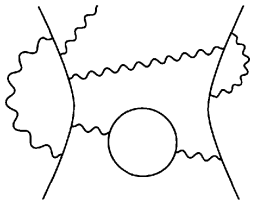

$$\sim \int \frac{d^4k_1\, d^4k_2 \cdots d^4k_L}{(\not{k}_i - m)\cdots(k_j^2)\cdots(k_n^2)}.$$

For each loop there is a potentially divergent 4-momentum integral, but each propagator aids the convergence of this integral by putting one or two powers of momentum into the denominator. Very roughly speaking, the diagram diverges unless there are more powers of momentum in the denominator than in the numerator. Let us therefore define the *superficial degree of divergence*, D, as the difference:

$$\begin{aligned} D &\equiv (\text{power of } k \text{ in numerator}) - (\text{power of } k \text{ in denominator}) \\ &= 4L - P_e - 2P_\gamma. \end{aligned} \tag{10.1}$$

Naively, we expect a diagram to have a divergence proportional to Λ^D, where Λ is a momentum cutoff, when $D > 0$. We expect a divergence of the form $\log\Lambda$ when $D = 0$, and no divergence when $D < 0$.

This naive expectation is often wrong, for one of three reasons (see Fig. 10.1). When a diagram contains a divergent subdiagram, its actual divergence may be worse than that indicated by D. When symmetries (such as the Ward identity) cause certain terms to cancel, the divergence of a diagram may be reduced or even eliminated. Finally, a trivial diagram with no propagators and no loops has $D = 0$ but no divergence.

Despite all of these complications, D is still a useful quantity. To see why, let us rewrite it in terms of the number of external lines (N_e, N_γ) and vertices (V). Note that the number of loop integrations in a diagram is

$$L = P_e + P_\gamma - V + 1, \tag{10.2}$$

since in our original Feynman rules each propagator has a momentum integral, each vertex has a delta function, and one delta function merely enforces overall momentum conservation. Furthermore, the number of vertices is

$$V = 2P_\gamma + N_\gamma = \tfrac{1}{2}(2P_e + N_e), \tag{10.3}$$

since each vertex involves exactly one photon line and two electron lines. (The propagators count twice since they have two ends on vertices.) Putting these relations together, we find that D can be expressed as

$$\begin{aligned} D &= 4(P_e + P_\gamma - V + 1) - P_e - 2P_\gamma \\ &= 4 - N_\gamma - \tfrac{3}{2}N_e, \end{aligned} \tag{10.4}$$

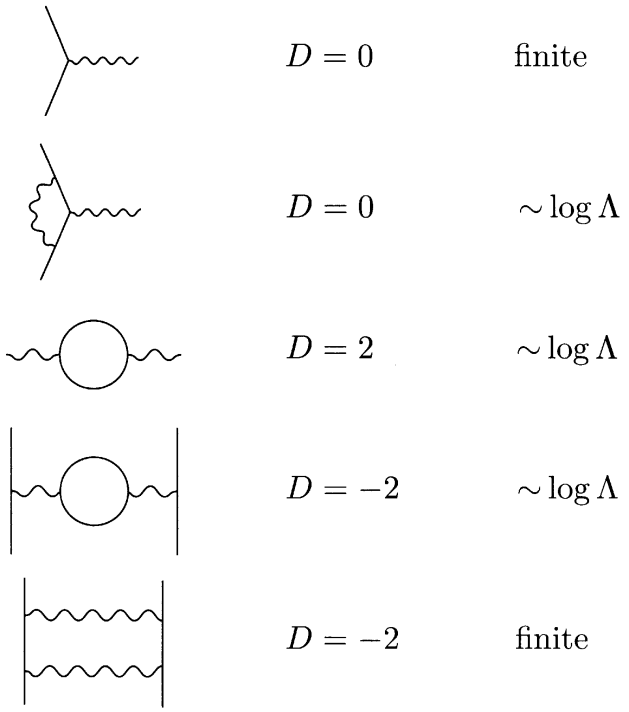

Figure 10.1. Some simple QED diagrams that illustrate the superficial degree of divergence. The first diagram is finite, even though $D = 0$. The third diagram has $D = 2$ but only a logarithmic divergence, due to the Ward identity (see Section 7.5). The fourth diagram diverges, even though $D < 0$, since it contains a divergent subdiagram. Only in the second and fifth diagrams does the superficial degree of divergence coincide with the actual degree of divergence.

independent of the number of vertices. The superficial degree of divergence of a QED diagram depends only on the number of external legs of each type.

According to result (10.4), only diagrams with a small number of external legs have $D \geq 0$; those seven types of diagrams are shown in Fig. 10.2. Since external legs do not enter the potentially divergent integral, we can restrict our attention to amputated diagrams. We can also restrict our attention to one-particle-irreducible diagrams, since reducible diagrams are simple products of the integrals corresponding to their irreducible parts. Thus the task of enumerating all of the divergent QED diagrams reduces to that of analyzing the seven types of amputated, one-particle-irreducible amplitudes shown in Fig. 10.2. Other diagrams may diverge, but only when they contain one of these seven as a subdiagram. Let us therefore consider each of these seven amplitudes in turn.

The zero-point function, Fig. 10.2a, is very badly divergent. But this object merely causes an unobservable shift of the vacuum energy; it never contributes to S-matrix elements.

To analyze the photon one-point function (Fig. 10.2b), note that the external photon must be attached to a QED vertex. Neglecting the external

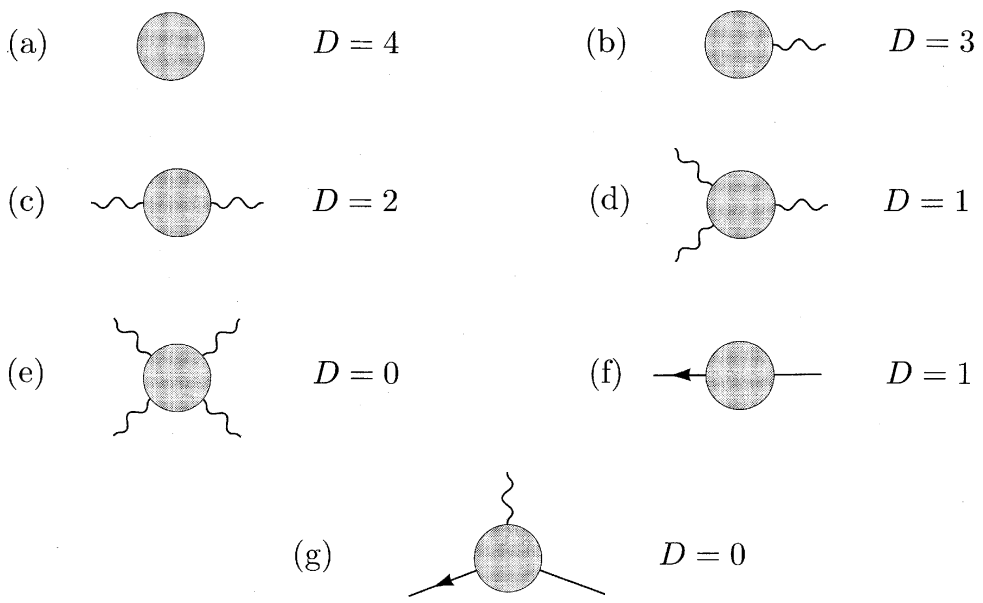

Figure 10.2. The seven QED amplitudes whose superficial degree of divergence (D) is ≥ 0. (Each circle represents the sum of all possible QED diagrams.) As explained in the text, amplitude (a) is irrelevant to scattering processes, while amplitudes (b) and (d) vanish because of symmetries. Amplitude (e) is nonzero, but its divergent parts cancel due to the Ward identity. The remaining amplitudes (c, f, and g) are all logarithmically divergent, even though $D > 0$ for (c) and (f).

photon propagator, this amplitude is therefore

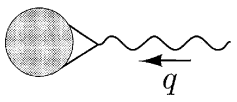

$$= -ie \int d^4x\, e^{-iq\cdot x} \langle \Omega | T\, j_\mu(x) | \Omega \rangle , \qquad (10.5)$$

where $j^\mu = \bar{\psi}\gamma^\mu\psi$ is the electromagnetic current operator. But the vacuum expectation value of j^μ must vanish by Lorentz invariance, since otherwise it would be a preferred 4-vector.

The photon one-point function also vanishes for a second reason: charge-conjugation invariance. Recall that C is a symmetry of QED, so $C|\Omega\rangle = |\Omega\rangle$. But $j^\mu(x)$ changes sign under charge conjugation, $Cj^\mu(x)C^\dagger = -j^\mu(x)$, so its vacuum expectation value must vanish:

$$\langle \Omega | T j^\mu(x) | \Omega \rangle = \langle \Omega | C^\dagger C j^\mu(x) C^\dagger C | \Omega \rangle = - \langle \Omega | T j^\mu(x) | \Omega \rangle = 0.$$

The same argument applies to any vacuum expectation value of an odd number of electromagnetic currents. In particular, the photon three-point function, Fig. 10.2d, vanishes. (This result is known as Furry's theorem.) It is not hard to check explicitly that the photon one- and three-point functions vanish in the leading order of perturbation theory (see Problem 10.1).

The remaining amplitudes in Fig. 10.2 are all nonzero, so we must analyze their structures in more detail. Consider, for example, the electron self-energy

(Fig. 10.2f). This amplitude is a function of the electron momentum p, so let us expand it in a Taylor series about $p = 0$:

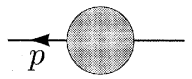

$$= A_0 + A_1 \not{p} + A_2 p^2 + \cdots ,$$

where each coefficient is independent of p:

$$A_n = \frac{1}{n!} \frac{d^n}{d\not{p}^n} \left(\quad \right) \Big|_{\not{p}=0} .$$

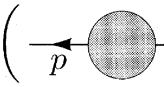

(These coefficients are infrared divergent; to compute them explicitly we would need an infrared regulator, as in Chapter 6.) The diagrams contributing to the electron self-energy depend on p through the denominators of propagators. To compute the coefficients A_n, we differentiate these propagators, giving expressions like

$$\frac{d}{d\not{p}} \left(\frac{1}{\not{k} + \not{p} - m} \right) = - \frac{1}{(\not{k} + \not{p} - m)^2} .$$

That is, each derivative with respect to the external momentum p lowers the superficial degree of divergence by 1. Since the constant term A_0 has (superficially) a linear divergence, A_1 can have only a logarithmic divergence; all the remaining A_n are finite. (This argument breaks down when the divergence is in a subdiagram, since then not all propagators involve the large momentum k. We will face this problem in Section 10.4.)

The electron self-energy amplitude has one additional subtlety. If the constant term A_0 were proportional to Λ (the ultraviolet cutoff), the electron mass shift would, according to the analysis in Section 7.1, also have a term proportional to Λ. But the electron mass shift must actually be proportional to m, since chiral symmetry would forbid a mass shift if m were zero. At worst, the constant term can be proportional to $m \log \Lambda$. We therefore expect the entire self-energy amplitude to have the form

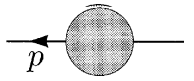

$$= a_0 m \log \Lambda + a_1 \not{p} \log \Lambda + (\text{finite terms}), \tag{10.6}$$

exactly what we found for the term of order α in Eq. (7.19).

Let us analyze the exact electron-photon vertex, Fig. 10.2g, in the same way. (Again we implicitly assume that infrared divergences have been regulated.) Expanding in powers of the three external momenta, we immediately see that only the constant term is divergent, since differentiating with respect to any external momentum would lower the degree of divergence to -1. This amplitude therefore contains only one divergent constant:

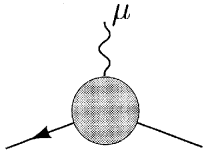

$$\propto -ie\gamma^\mu \log \Lambda + \text{finite terms}. \tag{10.7}$$

As discussed in Section 7.5, the photon self energy (Fig. 10.2c) is constrained by the Ward identity to have the form

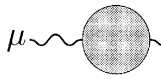

$$= (g^{\mu\nu}q^2 - q^\mu q^\nu)\Pi(q^2). \tag{10.8}$$

Viewing this expression as a Taylor series in q, we see that the constant and linear terms both vanish, lowering the superficial degree of divergence from 2 to 0. The only divergence, therefore, is in the constant term of $\Pi(q^2)$, and this divergence is only logarithmic. This result is exactly what we found for the lowest-order contribution to $\Pi(q^2)$ in Eq. (7.90).

Finally, consider the photon-photon scattering amplitude, Fig. 10.2e. The Ward identity requires that if we replace any external photon by its momentum vector, the amplitude vanishes:

k^μ 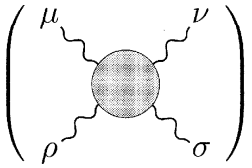

$$= 0. \tag{10.9}$$

By exhaustion one can show that this condition is satisfied only if the amplitude is proportional to $(g^{\mu\nu}k^\sigma - g^{\mu\sigma}k^\nu)$, with a similar factor for each of the other three legs. Each of these factors involves one power of momentum, so all terms with less than four powers of momentum in the Taylor series of this amplitude must vanish. The first nonvanishing term has $D = 0 - 4 = -4$, and therefore this amplitude is finite.

In summary, we have found that there are only three "primitively" divergent amplitudes in QED: the three that we already found in Chapters 6 and 7. (Other amplitudes may also be divergent, but only because of diagrams that contain these primitive amplitudes as components.) Furthermore, the dependence of these divergent amplitudes on external momenta is extremely simple. If we expand each amplitude as a power series in its external momenta, there are altogether only four divergent coefficients in the expansions. In other words, QED contains only four divergent numbers. In the next section we will see how these numbers can be absorbed into unobservable Lagrangian parameters, so that observable scattering amplitudes are always finite.

For the remainder of this section, let us try to understand the superficial degree of divergence from a more general viewpoint. The theory of QED in four spacetime dimensions is rather special, so let us first generalize to QED in d dimensions. In this case, D is given by

$$D \equiv dL - P_e - 2P_\gamma, \tag{10.10}$$

since each loop contributes a d-dimensional momentum integral. Relations (10.2) and (10.3) still hold, so we can again rewrite D in terms of V, N_e,

and N_γ. This time the result is

$$D = d + \left(\frac{d-4}{2}\right)V - \left(\frac{d-2}{2}\right)N_\gamma - \left(\frac{d-1}{2}\right)N_e. \tag{10.11}$$

The cancellation of V in this expression is special to the case $d = 4$. For $d < 4$, diagrams with more vertices have a lower degree of divergence, so the total number of divergent *diagrams* is finite. For $d > 4$, diagrams with more vertices have a higher degree of divergence, so every amplitude becomes superficially divergent at a sufficiently high order in perturbation theory.

These three possible types of ultraviolet behavior will also occur in other quantum field theories. We will refer to them as follows:

Super-Renormalizable theory:	Only a finite number of Feynman diagrams superficially diverge.
Renormalizable theory:	Only a finite number of amplitudes superficially diverge; however, divergences occur at all orders in perturbation theory.
Non-Renormalizable theory:	All amplitudes are divergent at a sufficiently high order in perturbation theory.

Using this nomenclature, we would say that QED is renormalizable in four dimensions, super-renormalizable in less than four dimensions, and non-renormalizable in more than four dimensions.

These superficial criteria give a correct picture of the true divergence structure of the theory for most cases that have been studied in detail. Examples are known in which the true behavior is better than this picture suggests, when powerful symmetries set to zero some or all of the superficially divergent amplitudes.* On the other hand, as we will explain in Section 10.4, it is always true that the divergences of superficially renormalizable theories can be absorbed into a finite number of Lagrangian parameters. For theories containing fields of spin 1 and higher, loop diagrams can produce additional problems, including violation of unitarity; we will discuss this difficulty in Chapter 16.

As another example of the counting of ultraviolet divergences, consider a pure scalar field theory, in d dimensions, with a ϕ^n interaction term:

$$\mathcal{L} = \frac{1}{2}(\partial_\mu\phi)^2 - \frac{1}{2}m^2\phi^2 - \frac{\lambda}{n!}\phi^n. \tag{10.12}$$

Let N be the number of external lines in a diagram, P the number of propagators, and V the number of vertices. The number of loops in a diagram is $L = P - V + 1$. There are n lines meeting at each vertex, so $nV = N + 2P$.

*Some exotic four-dimensional field theories are actually free of divergences; see, for example, the article by P. West in *Shelter Island II*, R. Jackiw, N. N. Khuri, S. Weinberg, and E. Witten, eds. (MIT Press, Cambridge, 1985).

Combining these relations, we find that the superficial degree of divergence of a diagram is

$$\begin{aligned} D &= dL - 2P \\ &= d + \left[n\left(\frac{d-2}{2}\right) - d\right]V - \left(\frac{d-2}{2}\right)N. \end{aligned} \tag{10.13}$$

In four dimensions a ϕ^4 coupling is renormalizable, while higher powers of ϕ are non-renormalizable. In three dimensions a ϕ^6 coupling becomes renormalizable, while ϕ^4 is super-renormalizable. In two spacetime dimensions any coupling of the form ϕ^n is super-renormalizable.

Expression (10.13) can also be derived in a somewhat different way, from dimensional analysis. In any quantum field theory, the action $S = \int d^d x\, \mathcal{L}$ must be dimensionless, since we work in units where $\hbar = 1$. In this system of units, the integral $d^d x$ has units $(\text{mass})^{-d}$, and so the Lagrangian has units $(\text{mass})^d$. Since all units can be expressed as powers of mass, it is unambiguous to say simply that the Lagrangian has "dimension d". Using this result, we can infer from the explicit form of (10.12) the dimensions of the field ϕ and the coupling constant λ. From the kinetic term in $\mathcal{L}$ we see that ϕ has dimension $(d-2)/2$. Note that the parameter m consistently has dimensions of mass. From the interaction term and the dimension of ϕ, we infer that the λ has dimension $d - n(d-2)/2$.

Now consider an arbitrary diagram with N external lines. One way that such a diagram could arise is from an interaction term $\eta\phi^N$ in the Lagrangian. The dimension of η would then be $d - N(d-2)/2$, and therefore we conclude that any (amputated) diagram with N external lines has dimension $d - N(d-2)/2$. In our theory with only the $\lambda\phi^n$ vertex, if the diagram has V vertices, its divergent part is proportional to $\lambda^V \Lambda^D$, where Λ is a high-momentum cutoff and D is the superficial degree of divergence. (This is the "generic" case; all the exceptions noted above also apply here.) Applying dimensional analysis, we find

$$d - N\left(\frac{d-2}{2}\right) = V\left[d - n\left(\frac{d-2}{2}\right)\right] + D,$$

in agreement with (10.13).

Note that the quantity that multiplies V in this expression is just the dimension of the coupling constant λ. This analysis can be carried out for QED and other field theories, with the same result. Thus we can characterize the three degrees of renormalizability in a second way:

Super-Renormalizable:	Coupling constant has positive mass dimension.
Renormalizable:	Coupling constant is dimensionless.
Non-Renormalizable:	Coupling constant has negative mass dimension.

This is exactly the conclusion that we stated without proof in Section 4.1. In QED, the coupling constant e is dimensionless; thus QED is (at least superficially) renormalizable.

10.2 Renormalized Perturbation Theory

In the previous section we saw that a renormalizable quantum field theory contains only a small number of superficially divergent amplitudes. In QED, for example, there are three such amplitudes, containing four infinite constants. In Chapters 6 and 7 these infinities disappeared by the end of our computations: The infinity in the vertex correction diagram was canceled by the electron field-strength renormalization, while the infinity in the vacuum polarization diagram caused only an unobservable shift of the electron's charge. In fact, it is generally true that the divergences in a renormalizable quantum field theory never show up in observable quantities.

To obtain a finite result for an amplitude involving divergent diagrams, we have so far used the following procedure: Compute the diagrams using a regulator, to obtain an expression that depends on the bare mass (m_0), the bare coupling constant (e_0), and some ultraviolet cutoff (Λ). Then compute the physical mass (m) and the physical coupling constant (e), to whatever order is consistent with the rest of the calculation; these quantities will also depend on m_0, e_0, and Λ. To calculate an S-matrix element (rather than a correlation function), one must also compute the field-strength renormalization(s) Z (in accord with Eq. (7.45)). Combining all of these expressions, eliminate m_0 and e_0 in favor of m and e; this step is the "renormalization". The resulting expression for the amplitude should be finite in the limit $\Lambda \to \infty$.

The above procedure always works in a renormalizable quantum field theory. However, it can often be cumbersome, especially at higher orders in perturbation theory. In this section we will develop an alternative procedure which works more automatically. We will do this first for ϕ^4 theory, returning to QED in the next section.

The Lagrangian of ϕ^4 theory is

$$\mathcal{L} = \frac{1}{2}(\partial_\mu \phi)^2 - \frac{1}{2}m_0^2\phi^2 - \frac{\lambda_0}{4!}\phi^4.$$

We now write m_0 and λ_0, to emphasize that these are the bare values of the mass and coupling constant, not the values measured in experiments.

The superficial degree of divergence of a diagram with N external legs is, according to (10.13),

$$D = 4 - N.$$

Since the theory is invariant under $\phi \to -\phi$, all amplitudes with an odd

number of external legs vanish. The only divergent amplitudes are therefore

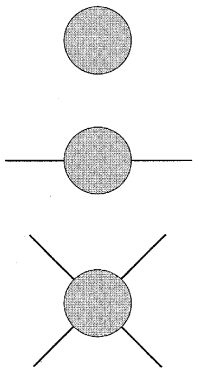

(unobservable vacuum energy shift);

$\sim\Lambda^2 + p^2 \log\Lambda +$ (finite terms);

$\sim \log\Lambda +$ (finite terms).

Ignoring the vacuum diagram, these amplitudes contain three infinite constants. Our goal is to absorb these constants into the three unobservable parameters of the theory: the bare mass, the bare coupling constant, and the field strength. To accomplish this goal, it is convenient to reformulate the perturbation expansion so that these unobservable quantities do not appear explicitly in the Feynman rules.

First we will eliminate the shift in the field strength. Recall from Section 7.1 that the exact two-point function has the form

$$\int d^4x\, \langle\Omega|\, T\phi(x)\phi(0)\, |\Omega\rangle\, e^{ip\cdot x} = \frac{iZ}{p^2 - m^2} + (\text{terms regular at } p^2 = m^2), \tag{10.14}$$

where m is the physical mass. We can eliminate the awkward residue Z from this equation by rescaling the field:

$$\phi = Z^{1/2}\phi_r. \tag{10.15}$$

This transformation changes the values of correlation functions by a factor of $Z^{-1/2}$ for each field. Thus, in computing S-matrix elements, we no longer need the factors of Z in Eq. (7.45); a scattering amplitude is simply the sum of all connected, amputated diagrams, exactly as we originally guessed in Eq. (4.103).

The Lagrangian is much uglier after the rescaling:

$$\mathcal{L} = \frac{1}{2}Z(\partial_\mu\phi_r)^2 - \frac{1}{2}m_0^2 Z\phi_r^2 - \frac{\lambda_0}{4!}Z^2\phi_r^4. \tag{10.16}$$

The bare mass and coupling constant still appear in $\mathcal{L}$, but they can be eliminated as follows. Define

$$\delta_Z = Z - 1, \qquad \delta_m = m_0^2 Z - m^2, \qquad \delta_\lambda = \lambda_0 Z^2 - \lambda, \tag{10.17}$$

where m and λ are the physically measured mass and coupling constant. Then the Lagrangian becomes

$$\begin{aligned}\mathcal{L} = {} & \frac{1}{2}(\partial_\mu\phi_r)^2 - \frac{1}{2}m^2\phi_r^2 - \frac{\lambda}{4!}\phi_r^4 \\ & + \frac{1}{2}\delta_Z(\partial_\mu\phi_r)^2 - \frac{1}{2}\delta_m\phi_r^2 - \frac{\delta_\lambda}{4!}\phi_r^4.\end{aligned} \tag{10.18}$$

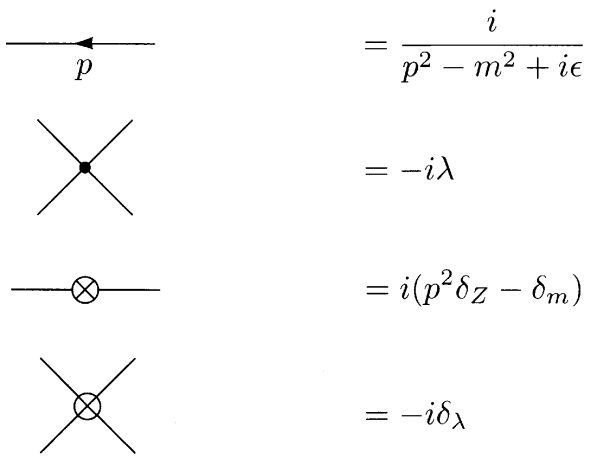

Figure 10.3. Feynman rules for ϕ^4 theory in renormalized perturbation theory.

The first line now looks like the familiar ϕ^4-theory Lagrangian, but is written in terms of the physical mass and coupling. The terms in the second line, known as *counterterms*, have absorbed the infinite but unobservable shifts between the bare parameters and the physical parameters. It is tempting to say that we have "added" these counterterms to the Lagrangian, but in fact we have merely split each term in (10.16) into two pieces.

The definitions in (10.17) are not useful unless we give precise definitions of the physical mass and coupling constant. Equation (10.14) defines m^2 as the location of the pole in the propagator. There is no obviously best definition of λ, but a perfectly good definition would be obtained by setting λ equal to the magnitude of the scattering amplitude at zero momentum. Thus we have the two defining relations,

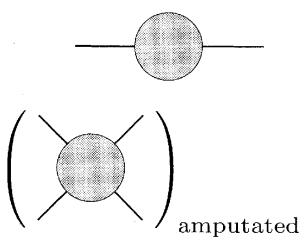

$$= \frac{i}{p^2 - m^2} + (\text{terms regular at } p^2 = m^2);$$

$$= -i\lambda \qquad \text{at } s = 4m^2,\ t = u = 0. \tag{10.19}$$

These equations are called *renormalization conditions*. (The first equation actually contains two conditions, specifying both the location of the pole and its residue.)

Our new Lagrangian, Eq. (10.18), gives a new set of Feynman rules, shown in Fig. 10.3. The propagator and the first vertex come from the first line of (10.18), and are identical to the old rules except for the appearance of the physical mass and coupling in place of the bare values. The counterterms in the second line of (10.18) give two new vertices (also called counterterms).

We can use these new Feynman rules to compute any amplitude in ϕ^4 theory. The procedure is as follows. Compute the desired amplitude as the sum of all possible diagrams created from the propagator and vertices shown

in Fig. 10.3. The loop integrals in the diagrams will often diverge, so one must introduce a regulator. The result of this computation will be a function of the three unknown parameters δ_Z, δ_m, and δ_λ. Adjust (or "renormalize") these three parameters as necessary to maintain the renormalization conditions (10.19). After this adjustment, the expression for the amplitude should be finite and independent of the regulator.

This procedure, using Feynman rules with counterterms, is known as *renormalized perturbation theory.* It should be contrasted with the procedure we used in Part 1, outlined at the beginning of this section, which is called *bare perturbation theory* (since the Feynman rules involve the bare mass and coupling constant). The two methods are completely equivalent. The differences between them are purely a matter of bookkeeping. You will get the same answers using either procedure, so you may choose whichever you find more convenient. In general, renormalized perturbation theory is technically easier to use, especially for multiloop diagrams; however, bare perturbation theory is sometimes easier for complicated one-loop calculations. We will use renormalized perturbation theory in most of the rest of this book.

One-Loop Structure of ϕ^4 Theory

To make more sense of the renormalization procedure, let us carry it out explicitly at the one-loop level.

First consider the basic two-particle scattering amplitude,

$i\mathcal{M}(p_1p_2 \to p_3p_4) =$

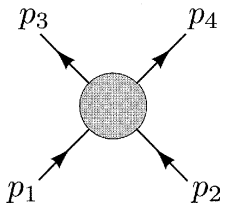

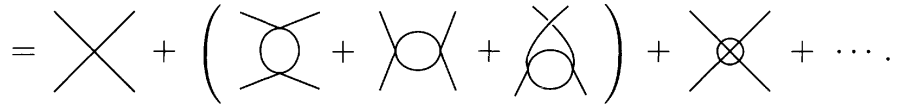

If we define $p = p_1 + p_2$, then the second diagram is

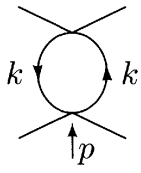

$$= \frac{(-i\lambda)^2}{2} \int \frac{d^4k}{(2\pi)^4} \frac{i}{k^2 - m^2} \frac{i}{(k+p)^2 - m^2}$$

$$\equiv (-i\lambda)^2 \cdot iV(p^2). \tag{10.20}$$

Note that p^2 is equal to the Mandelstam variable s. The next two diagrams are identical, except that s will be replaced by t and u. The entire amplitude is therefore

$$i\mathcal{M} = -i\lambda + (-i\lambda)^2\big[iV(s) + iV(t) + iV(u)\big] - i\delta_\lambda. \tag{10.21}$$

According to our renormalization condition (10.19), this amplitude should

equal $-i\lambda$ at $s = 4m^2$ and $t = u = 0$. We must therefore set

$$\delta_\lambda = -\lambda^2 \big[V(4m^2) + 2V(0)\big]. \tag{10.22}$$

(At higher orders, δ_λ will receive additional contributions.)

We can compute $V(p^2)$ explicitly using dimensional regularization. The procedure is exactly the same as in Section 7.5: Introduce a Feynman parameter, shift the integration variable, rotate to Euclidean space, and perform the momentum integral. We obtain

$$\begin{aligned}
V(p^2) &= \frac{i}{2}\int_0^1 dx \int \frac{d^dk}{(2\pi)^d} \frac{1}{\big[k^2 + 2xk\cdot p + xp^2 - m^2\big]^2} \\
&= \frac{i}{2}\int_0^1 dx \int \frac{d^d\ell}{(2\pi)^d} \frac{1}{\big[\ell^2 + x(1-x)p^2 - m^2\big]^2} \qquad (\ell = k + xp) \\
&= -\frac{1}{2}\int_0^1 dx \int \frac{d^d\ell_E}{(2\pi)^d} \frac{1}{\big[\ell_E^2 - x(1-x)p^2 + m^2\big]^2} \qquad (\ell_E^0 = -i\ell^0) \\
&= -\frac{1}{2}\int_0^1 dx \frac{\Gamma(2-\frac{d}{2})}{(4\pi)^{d/2}} \frac{1}{\big[m^2 - x(1-x)p^2\big]^{2-d/2}} \\
&\xrightarrow[d\to 4]{} -\frac{1}{32\pi^2}\int_0^1 dx \Big(\frac{2}{\epsilon} - \gamma + \log(4\pi) - \log\big[m^2 - x(1-x)p^2\big]\Big),
\end{aligned} \tag{10.23}$$

where $\epsilon = 4 - d$. The shift in the coupling constant (10.22) is therefore

$$\begin{aligned}
\delta_\lambda &= \frac{\lambda^2}{2}\frac{\Gamma(2-\frac{d}{2})}{(4\pi)^{d/2}}\int_0^1 dx \Big(\frac{1}{[m^2 - x(1-x)4m^2]^{2-d/2}} + \frac{2}{[m^2]^{2-d/2}}\Big) \\
&\xrightarrow[d\to 4]{} \frac{\lambda^2}{32\pi^2}\int_0^1 dx \Big(\frac{6}{\epsilon} - 3\gamma + 3\log(4\pi) - \log\big[m^2 - x(1-x)4m^2\big] - 2\log\big[m^2\big]\Big).
\end{aligned} \tag{10.24}$$

These expressions are divergent as $d \to 4$. But if we combine them according to (10.21), we obtain the finite (if rather complicated) result,

$$\begin{aligned}
i\mathcal{M} = -i\lambda - \frac{i\lambda^2}{32\pi^2}\int_0^1 dx \Big[&\log\Big(\frac{m^2 - x(1-x)s}{m^2 - x(1-x)4m^2}\Big) + \log\Big(\frac{m^2 - x(1-x)t}{m^2}\Big) \\
&+ \log\Big(\frac{m^2 - x(1-x)u}{m^2}\Big)\Big].
\end{aligned} \tag{10.25}$$

To determine δ_Z and δ_m we must compute the two-point function. As in Section 7.2, let us define $-iM^2(p^2)$ as the sum of all one-particle-irreducible insertions into the propagator:

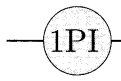

$$= -iM^2(p^2). \tag{10.26}$$

Then the full two-point function is given by the geometric series,

$$= \frac{i}{p^2 - m^2 - M^2(p^2)}. \tag{10.27}$$

The renormalization conditions (10.19) require that the pole in this full propagator occur at $p^2 = m^2$ and have residue 1. These two conditions are equivalent, respectively, to

$$M^2(p^2)\big|_{p^2=m^2} = 0 \qquad \text{and} \qquad \frac{d}{dp^2} M^2(p^2)\big|_{p^2=m^2} = 0. \tag{10.28}$$

(To check the latter condition, expand M^2 about $p^2 = m^2$ in Eq. (10.27).)

Explicitly, to one-loop order,

$$-iM^2(p^2) =$$

$$= -i\lambda \cdot \frac{1}{2} \cdot \int \frac{d^dk}{(2\pi)^d} \frac{i}{k^2 - m^2} + i(p^2\delta_Z - \delta_m)$$

$$= -\frac{i\lambda}{2} \frac{1}{(4\pi)^{d/2}} \frac{\Gamma(1-\frac{d}{2})}{(m^2)^{1-d/2}} + i(p^2\delta_Z - \delta_m). \tag{10.29}$$

Since the first term is independent of p^2, the result is rather trivial: Setting

$$\delta_Z = 0 \qquad \text{and} \qquad \delta_m = -\frac{\lambda}{2(4\pi)^{d/2}} \frac{\Gamma(1-\frac{d}{2})}{(m^2)^{1-d/2}} \tag{10.30}$$

yields $M^2(p^2) = 0$ for all p^2, satisfying both of the conditions in (10.28).

The first nonzero contributions to $M^2(p^2)$ and δ_Z are proportional to λ^2, coming from the diagrams

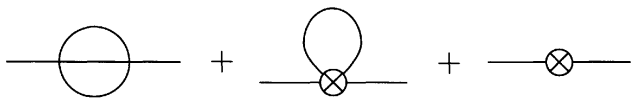

(10.31)

The second diagram contains the δ_λ counterterm, which we have already computed. It cancels ultraviolet divergences in the first diagram that occur when one of the loop momenta is large and the other is small. The third diagram is again the $(p^2\delta_Z - \delta_m)$ counterterm, and is fixed to order λ^2 by requiring

that the remaining divergences (when both loop momenta become large) cancel. In Section 10.4 we will see an explicit example of the interplay of various counterterms in a two-loop calculation.

The vanishing of δ_Z at one-loop order is a special feature of ϕ^4 theory, which does not occur in more general theories of scalar fields. The Yukawa theory described in Section 4.7 gives an explicit example of a one-loop correction for which this counterterm is required.

In the Yukawa theory, the scalar field propagator receives corrections at order g^2 from a fermion loop diagram and the two propagator counterterms. Using the Feynman rules on p. 118 to compute the loop diagram, we find

$$-iM^2(p^2) = \quad \overset{p}{\text{---}}\!\!\bigcirc\!\!\!\!\begin{matrix}k+p\\ \\ k\end{matrix}\!\!\text{---} \quad + \quad \text{---}\otimes\text{---}$$

$$= -(-ig)^2 \int \frac{d^dk}{(2\pi)^d} \operatorname{tr}\left[\frac{i(\not{k}+\not{p}+m_f)}{(k+p)^2-m_f^2}\,\frac{i(\not{k}+m_f)}{k^2-m_f^2}\right] + i(p^2\delta_Z - \delta_m)$$

$$= -4g^2 \int \frac{d^dk}{(2\pi)^d}\,\frac{k\cdot(p+k)+m_f^2}{((p+k)^2-m_f^2)(k^2-m_f^2)} + i(p^2\delta_Z-\delta_m), \quad (10.32)$$

where m_f is the mass of the fermion that couples to the Yukawa field. To evaluate the integral, combine denominators and shift as in Eq. (10.23). Then the first term in the last line becomes

$$-4g^2 \int_0^1 dx \int \frac{d^d\ell}{(2\pi)^d}\,\frac{\ell^2 - x(1-x)p^2 + m_f^2}{(\ell^2 + x(1-x)p^2 - m_f^2)^2}$$

$$= -4g^2 \int_0^1 dx\,\frac{-i}{(4\pi)^{d/2}}\left(\frac{\frac{d}{2}\Gamma(1-\frac{d}{2})}{\Delta^{1-d/2}} - \frac{\Delta\,\Gamma(2-\frac{d}{2})}{\Delta^{2-d/2}}\right)$$

$$= \frac{4ig^2(d-1)}{(4\pi)^{d/2}} \int_0^1 dx\,\frac{\Gamma(1-\frac{d}{2})}{\Delta^{1-d/2}}, \quad (10.33)$$

where $\Delta = m_f^2 - x(1-x)p^2$.

Now we can see that both of the counterterms δ_m and δ_Z must take nonzero values in order to satisfy the renormalization conditions (10.28). To determine δ_m, we subtract the value of the loop diagram at $p^2 = m^2$ as before, so that

$$\delta_m = \frac{4g^2(d-1)}{(4\pi)^{d/2}} \int_0^1 dx\,\frac{\Gamma(1-\frac{d}{2})}{[m_f^2 - x(1-x)m^2]^{1-d/2}} + m^2\delta_Z. \quad (10.34)$$

To determine δ_Z, we cancel also the first derivative with respect to p^2 of the

loop integral (10.33). This gives

$$\delta_Z = -\frac{4g^2(d-1)}{(4\pi)^{d/2}} \int_0^1 dx \, \frac{x(1-x)\Gamma(2-\frac{d}{2})}{[m_f^2 - x(1-x)m^2]^{2-d/2}}$$

$$\xrightarrow[d\to 4]{} -\frac{3g^2}{4\pi^2} \int_0^1 dx\, x(1-x)\left(\frac{2}{\epsilon} - \gamma - \frac{2}{3} + \log(4\pi) - \log\left[m_f^2 - x(1-x)m^2\right]\right). \tag{10.35}$$

Thus, in Yukawa theory, the propagator corrections at one-loop order require a quadratically divergent mass renormalization and a logarithmically divergent field strength renormalization. This is the usual situation in scalar field theories.

10.3 Renormalization of Quantum Electrodynamics

The procedure we followed in the previous section, yielding a "renormalized" perturbation theory formulated in terms of physically measurable parameters, can be summarized as follows:

1. Absorb the field-strength renormalizations into the Lagrangian by rescaling the fields.
2. Split each term of the Lagrangian into two pieces, absorbing the infinite and unobservable shifts into counterterms.
3. Specify the renormalization conditions, which define the physical masses and coupling constants and keep the field-strength renormalizations equal to 1.
4. Compute amplitudes with the new Feynman rules, adjusting the counterterms as necessary to maintain the renormalization conditions.

Let us now use this procedure to construct a renormalized perturbation theory for Quantum Electrodynamics.

The original QED Lagrangian is

$$\mathcal{L} = -\tfrac{1}{4}(F_{\mu\nu})^2 + \bar{\psi}(i\partial\!\!\!/ - m_0)\psi - e_0\bar{\psi}\gamma^\mu\psi A_\mu.$$

Computing the electron and photon propagators with this Lagrangian, we would find expressions of the general form

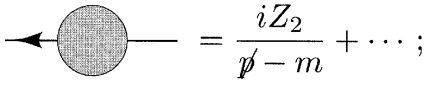

$$= \frac{iZ_2}{p\!\!\!/ - m} + \cdots;$$

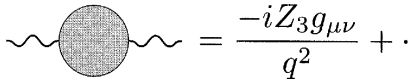

$$= \frac{-iZ_3 g_{\mu\nu}}{q^2} + \cdots.$$

(We found just such expressions in the explicit one-loop calculations of Chapter 7.) To absorb Z_2 and Z_3 into $\mathcal{L}$, and hence eliminate them from formula (7.45) for the S-matrix, we substitute $\psi = Z_2^{1/2}\psi_r$ and $A^\mu = Z_3^{1/2}A_r^\mu$. Then the Lagrangian becomes

$$\mathcal{L} = -\tfrac{1}{4}Z_3(F_r^{\mu\nu})^2 + Z_2\bar{\psi}_r(i\partial\!\!\!/ - m_0)\psi_r - e_0 Z_2 Z_3^{1/2}\bar{\psi}_r\gamma^\mu\psi_r A_{r\mu}. \tag{10.36}$$

We can introduce the physical electric charge e, measured at large distances ($q = 0$), by defining a scaling factor Z_1 as follows:[†]

$$e_0 Z_2 Z_3^{1/2} = e Z_1. \tag{10.37}$$

If we let m be the physical mass (the location of the pole in the electron propagator), then we can split each term of the Lagrangian into two pieces as follows:

$$\begin{aligned}\mathcal{L} = &-\tfrac{1}{4}(F_r^{\mu\nu})^2 + \bar{\psi}_r(i\partial\!\!\!/ - m)\psi_r - e\bar{\psi}_r\gamma^\mu\psi_r A_{r\mu} \\ &- \tfrac{1}{4}\delta_3(F_r^{\mu\nu})^2 + \bar{\psi}_r(i\delta_2\partial\!\!\!/ - \delta_m)\psi_r - e\delta_1\bar{\psi}_r\gamma^\mu\psi_r A_{r\mu},\end{aligned} \tag{10.38}$$

where

$$\delta_3 = Z_3 - 1, \qquad \delta_2 = Z_2 - 1,$$

$$\delta_m = Z_2 m_0 - m, \qquad \text{and} \qquad \delta_1 = Z_1 - 1 = (e_0/e)Z_2 Z_3^{1/2} - 1.$$

The Feynman rules for renormalized QED are shown in Fig. 10.4. In addition to the familiar propagators and vertex, there are three counterterm vertices. The ee and $ee\gamma$ counterterm vertices can be read directly from the Lagrangian (10.38). To derive the two-photon counterterm, integrate $-\frac{1}{4}(F_{\mu\nu})^2$ by parts to obtain $-\frac{1}{2}A_\mu(-\partial^2 g^{\mu\nu} + \partial^\mu\partial^\nu)A_\nu$; this gives the expression shown in the figure. In the remainder of the book, when we set up renormalized perturbation theory, we will drop the subscript r used here to distinguish the rescaled fields.

Each of the four counterterm coefficients must be fixed by a renormalization condition. The four conditions that we require have already been stated implicitly: Two of them fix the electron and photon field-strength renormalizations to 1, while the other two define the physical electron mass and charge. To write these conditions more explicitly, recall our notation from Chapters 6 and 7:

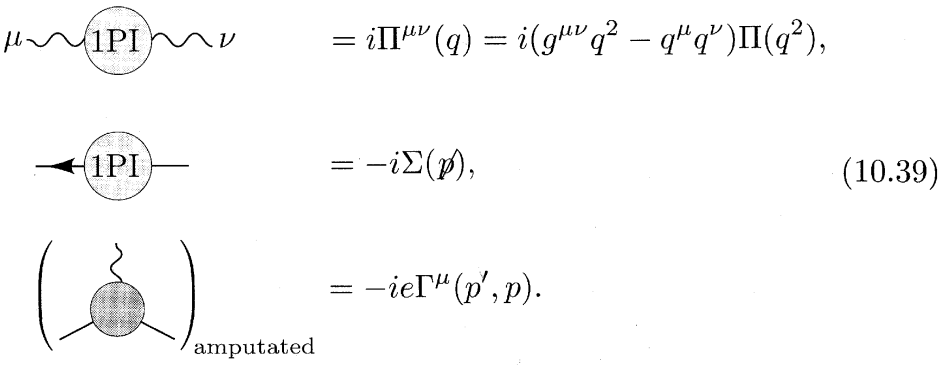

(10.39)

[†]Since we define e by the renormalization condition $\Gamma^\mu(q = 0) = \gamma^\mu$, the factor of Z_1 in the Lagrangian must cancel the multiplicative correction factor that arises from loop corrections. Therefore this definition of Z_1 is equivalent to that given in Eq. (7.47).

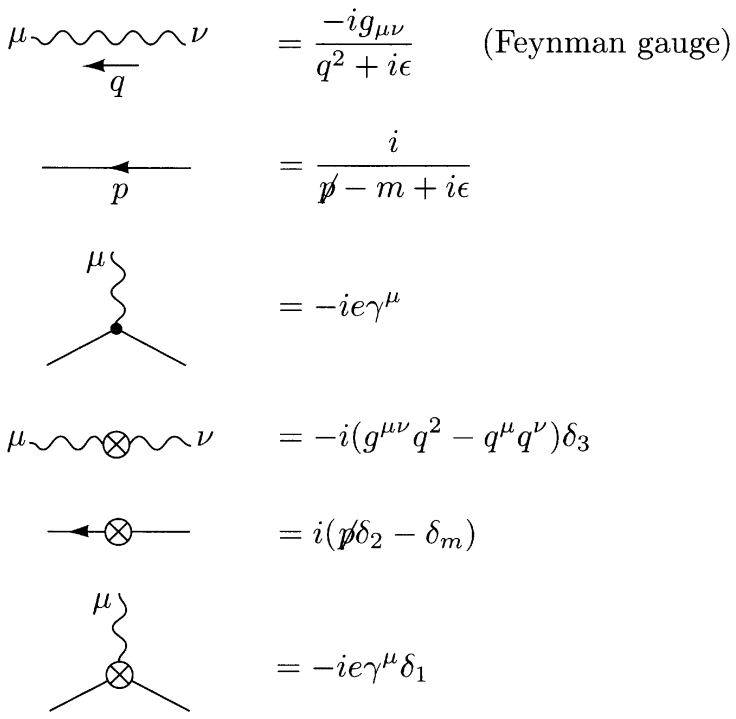

Figure 10.4. Feynman rules for Quantum Electrodynamics in renormalized perturbation theory.

These amplitudes are now to be computed in renormalized perturbation theory; that is, we are now redefining $\Pi(q^2)$, $\Sigma(\not{p})$, and $\Gamma(p', p)$ to include counterterm vertices. Furthermore, the new definition of Γ involves the physical electron charge. With this notation, the four conditions are

$$\begin{aligned} \Sigma(\not{p} = m) &= 0; \\ \frac{d}{d\not{p}}\Sigma(\not{p})\Big|_{\not{p}=m} &= 0; \\ \Pi(q^2 = 0) &= 0; \\ -ie\Gamma^\mu(p' - p = 0) &= -ie\gamma^\mu. \end{aligned} \tag{10.40}$$

The first condition fixes the electron mass at m, while the next two fix the residues of the electron and photon propagators at 1. Given these conditions, the final condition fixes the electron charge to be e.

One-Loop Structure of QED

The four conditions (10.40) allow us to determine the four countertems in (10.38) in terms of the values of loop diagrams. In Chapters 6 and 7 we computed all of the diagrams required to carry out this determination to one-loop order. We will now collect these results and find explicit expressions for the renormalization constants of QED to order α. For overall consistency, we will

use dimensional regularization to control ultraviolet divergences, and a photon mass μ to control infrared divergences. In Part I, we computed the vertex and self-energy diagrams using the Pauli-Villars regularization scheme, before introducing dimensional regularization. Now we have an opportunity to quote the values of these diagrams as computed with dimensional regularization.

The first two conditions involve the electron self-energy. We evaluated the one-loop diagram contributing to $\Sigma(p)$, using a Pauli-Villars regulator, in Section 7.1; the result is given in Eq. (7.19). If we re-evaluate the diagram in dimensional regularization, we find some additional terms in the Dirac algebra from the modified contraction identities (7.89). Taking these terms into account, we find for this diagram ($\epsilon = 4 - d$)

$$-i\Sigma_2(p) = -i\frac{e^2}{(4\pi)^{d/2}} \int_0^1 dx \, \frac{\Gamma(2-\frac{d}{2})}{((1-x)m^2 + x\mu^2 - x(1-x)p^2)^{2-d/2}} \times ((4-\epsilon)m - (2-\epsilon)x\not{p}). \tag{10.41}$$

Therefore, according to the first of conditions (10.40),

$$m\delta_2 - \delta_m = \Sigma_2(m) = \frac{e^2 m}{(4\pi)^{d/2}} \int_0^1 dx \, \frac{\Gamma(2-\frac{d}{2}) \cdot (4 - 2x - \epsilon(1-x))}{((1-x)^2 m^2 + x\mu^2)^{2-d/2}}. \tag{10.42}$$

Similarly, the second of conditions (10.40) determines δ_2:

$$\begin{aligned} \delta_2 &= \frac{d}{d\not{p}} \Sigma_2(m) \\ &= -\frac{e^2}{(4\pi)^{d/2}} \int_0^1 dx \, \frac{\Gamma(2-\frac{d}{2})}{((1-x)^2 m^2 + x\mu^2)^{2-d/2}} \\ &\quad \times \left[(2-\epsilon)x - \frac{\epsilon}{2} \frac{2x(1-x)m^2}{(1-x)^2 m^2 + x\mu^2} (4 - 2x - \epsilon(1-x)) \right]. \end{aligned} \tag{10.43}$$

Notice that the second term in the brackets gives a finite result as $\epsilon \to 0$, because it multiplies the divergent gamma function.

The third condition of (10.40) requires the value (7.90) of the photon self-energy diagram:

$$\Pi_2(q^2) = -\frac{e^2}{(4\pi)^{d/2}} \int_0^1 dx \, \frac{\Gamma(2-\frac{d}{2})}{(m^2 - x(1-x)q^2)^{2-d/2}} \big(8x(1-x)\big).$$

Then

$$\delta_3 = \Pi_2(0) = -\frac{e^2}{(4\pi)^{d/2}} \int_0^1 dx \, \frac{\Gamma(2-\frac{d}{2})}{(m^2)^{2-d/2}} \big(8x(1-x)\big). \tag{10.44}$$

The last condition requires the value of the electron vertex function, computed in Section 6.3. Again, we will rework the diagram in dimensional regularization. Then the shift in the form factor $F_1(q^2)$ (6.56) becomes

$$\delta F_1(q^2) = \frac{e^2}{(4\pi)^{d/2}} \int dx\, dy\, dz\, \delta(x+y+z-1) \left[\frac{\Gamma(2-\frac{d}{2})}{\Delta^{2-d/2}} \frac{(2-\epsilon)^2}{2} + \frac{\Gamma(3-\frac{d}{2})}{\Delta^{3-d/2}} \left(q^2[2(1-x)(1-y) - \epsilon xy] + m^2[2(1-4z+z^2) - \epsilon(1-z)^2] \right) \right], \tag{10.45}$$

where $\Delta = (1-z)^2 m^2 + z\mu^2 - xyq^2$ as before. The fourth renormalization condition then determines

$$\delta_1 = -\delta F_1(0) = -\frac{e^2}{(4\pi)^{d/2}} \int dz\, (1-z) \left[\frac{\Gamma(2-\frac{d}{2})}{((1-z)^2 m^2 + z\mu^2)^{2-d/2}} \frac{(2-\epsilon)^2}{2} + \frac{\Gamma(3-\frac{d}{2})}{((1-z)^2 m^2 + z\mu^2)^{3-d/2}} [2(1-4z+z^2) - \epsilon(1-z)^2] m^2 \right]. \tag{10.46}$$

Using an integration by parts similar to that following Eq. (7.32), one can show explicitly from (10.46) and (10.43) that $\delta_1 = \delta_2$, that is, that $Z_1 = Z_2$ to order α. As in our previous derivations, this formula follows from the Ward identity. The Lagrangian (10.38), with counterterms set to zero, is gauge invariant. If the regulator is also gauge invariant (and we do use dimensional regularization), this implies the Ward identity for diagrams without counterterm vertices. In particular, this implies that $\delta F_1(0) = -d\Sigma_2/d\not{p}|_m$. Then the counterterms δ_1 and δ_2, which are required to cancel these two factors, will be set equal.

By continuing this argument, it is straightforward to construct a full diagrammatic proof that $\delta_1 = \delta_2$, to all orders in renormalized perturbation theory, using the method we applied in Section 7.4 to prove the Ward-Takahashi identity in bare perturbation theory. With a generalization of the argument given there, one can show that the diagrammatic identity (7.68) holds for diagrams that include counterterm vertices in loops. Thus, if the counterterms δ_1 and δ_2 are determined up to order α^n, the unrenormalized vertex diagram at $q^2 = 0$ equals the derivative of the unrenormalized self-energy diagram on-shell in order α^{n+1}. To satisfy the renormalization conditions (10.40), we must then set the counterterms δ_1 and δ_2 equal to order α^{n+1}. This recursive argument gives yet another proof that $Z_1 = Z_2$ to all orders in QED perturbation theory.

The relation (10.37) between the bare and renormalized charge

$$e = \frac{Z_2}{Z_1} Z_3^{1/2}\, e_0 \tag{10.47}$$

gives a further physical interpretation of the identity $Z_1 = Z_2$. Using the identity, we can rewrite (10.47) as

$$e = \sqrt{Z_3} e_0,$$

which is just the relation (7.76) that we derived by a diagrammatic argument in Section 7.5. This says that the relation between the bare and renormalized electric charge depends only on the photon field strength renormalization, not on quantities particular to the electron. To see the importance of this observation, consider writing the renormalized quantum electrodynamics with two species of charged particles, say, electrons and muons. Then, in addition to (10.37), we will have a relation for the photon-muon vertex:

$$e Z_2'^{-1} Z_3^{-1/2} = e_0 Z_1'^{-1}, \tag{10.48}$$

where Z_1' and Z_2' are the vertex and field strength renormalizations for the muon. Each of these two constants depends on the mass of the muon, so (10.48) threatens to give a different relation between e_0 and e from the one written in (10.47). However, the Ward identity forces the factors Z_1' and Z_2' to cancel out of this relation, leaving over a universal electric charge which has the same value for all species.

10.4 Renormalization Beyond the Leading Order

In the last two sections we have developed an algorithm for computing scattering amplitudes to any order in a renormalizable field theory. We have seen explicitly that this algorithm yields finite results at the one-loop level in both ϕ^4 theory and QED. According to the naive analysis of Section 10.1, the algorithm should also work at higher orders. But that analysis ignored many of the intricacies of multiloop diagrams; specifically, it ignored the fact that diagrams can contain divergent subdiagrams.

When an otherwise finite diagram contains a divergent subdiagram, the treatment of the divergence is relatively straightforward. For example, the sum of diagrams

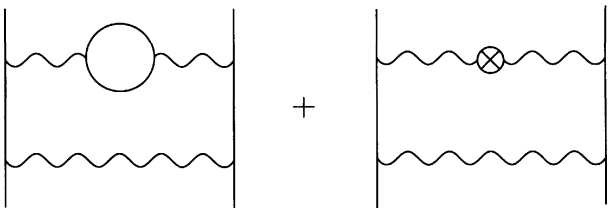

(10.49)

is finite: The divergence in the photon propagator cancels just as when this propagator occurs in a tree diagram. The finite sum of the two propagator

diagrams gives an integrand for the outer loop that falls off fast enough that this integral still converges.

A more difficult situation occurs when we have *nested* or *overlapping* divergences, that is, when two divergent loops share a propagator. Some examples of diagrams with overlapping divergences are

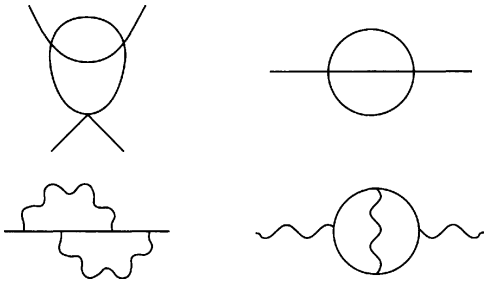

in ϕ^4 theory;

in QED.

To see the difficulty, consider the photon self-energy diagram:

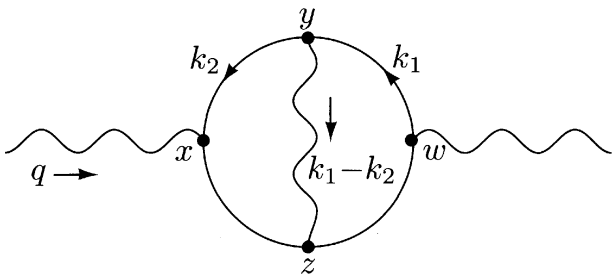

One contribution to this diagram comes from the region of momentum space where k_2 is very large. This means that, in position space, x, y, and z are very close together, while w can be farther away. In this region we can think of the virtual photon as giving a correction to the vertex at x. We saw in Section 6.3 that this vertex correction is logarithmically divergent, of the form

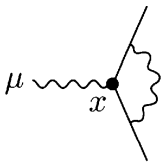

$$\sim -ie\gamma^\mu \cdot \alpha \log \Lambda^2$$

in the limit $\Lambda \to \infty$. Plugging this vertex into the rest of the diagram and integrating over k_1, we obtain an expression identical to the one-loop photon self-energy correction $\Pi_2(q^2)$, displayed in (7.90), multiplied by the additional logarithmic divergence:

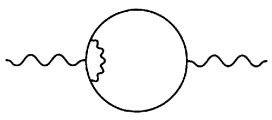

$$\begin{aligned} &\sim \alpha(g^{\mu\nu}q^2 - q^\mu q^\nu)\Pi_2(q^2) \cdot \alpha \log \Lambda^2 \\ &\sim \alpha(g^{\mu\nu}q^2 - q^\mu q^\nu)(\log \Lambda^2 + \log q^2) \cdot \alpha \log \Lambda^2. \end{aligned} \tag{10.50}$$

The $\log^2 \Lambda^2$ term comes from the region where both k_1 and k_2 are large, while the $\log q^2 \log \Lambda^2$ term comes from the region where k_2 is large but k_1 is small. Another such term would come from the region where k_1 is large but k_2 is small.

The appearance of terms proportional to $\Pi_2(q^2) \cdot \log \Lambda^2$ in the two-loop vacuum polarization diagram contradicts our naive argument, based on the criterion of the superficial degree of divergence, that the divergent terms of a Feynman integral are always simple polynomials in q^2. We will refer to divergences multiplying only polynomials in q^2 as *local divergences*, since their Fourier transforms back to position space are delta functions or derivatives of delta functions. We will call the new, nonpolynomial, term a *nonlocal* divergence. Fortunately, our derivation of the nonlocal divergent term gave this term a physical interpretation: It is a local divergence surrounded by an ordinary, nondivergent, quantum field theory process.

If this picture accurately describes all of the divergent terms of the two-loop diagram, we should expect that these divergences are canceled by two types of counterterm diagrams. First, we can build diagrams of order α^2 by inserting the order-α counterterm vertex into the one-loop vacuum polarization diagram:

These diagrams should cancel the nonlocal divergence in (10.50) and the corresponding contribution from the region where k_1 is large and k_2 is small. In fact, a detailed analysis shows that the sum of the original diagram and these two counterterm diagrams contains only local divergences. Once these diagrams are added, the only divergence that remains is a local one, which can be canceled by the diagram

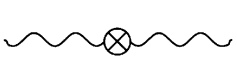

that is, by adding an order-α^2 term to δ_3.

We can extend the lessons of this example to a general picture of the divergences of higher-loop Feynman diagrams and their cancellation. A given diagram may contain local divergences, as predicted by the analysis of Section 10.1. It may also contain nonlocal divergences due to divergent subgraphs embedded in loops carrying small momenta. These divergences are canceled by diagrams in which the divergent subgraphs are replaced by their counterterm vertices. One might still ask two questions: First, does this procedure remove all nonlocal divergences? Second, does this procedure preserve the finiteness of amplitudes, such as (10.49), that are not expected to be divergent by the superficial criteria of Section 10.1? To answer these questions requires an intricate study of nested Feynman integrals. The general analysis was begun by Bogoliubov and Parasiuk, completed by Hepp, and elegantly refined by

Zimmermann;[‡] they showed that the answer to both questions is yes. Their result, known as the BPHZ theorem, states that, for a general renormalizable quantum field theory, to any order in perturbation theory, all divergences are removed by the counterterm vertices corresponding to superficially divergent amplitudes. In other words, any superficially renormalizable quantum field theory is in fact rendered finite when one performs renormalized perturbation theory with the complete set of counterterms.

The proof of the BPHZ theorem is quite technical, and we will not include it in this book. Instead, we will investigate one detailed example of a two-loop calculation, which demonstrates explicitly the appearance and cancellation of nonlocal divergences.

10.5 A Two-Loop Example

To illustrate the issues discussed in the previous section, let us consider the two-loop contribution to the four-point function in ϕ^4 theory. There are 16 relevant diagrams, shown in Fig. 10.5. (There are also several diagrams involving the one-loop correction to the propagator. But each of these is exactly canceled by its counterterm, as we saw in Eq. (10.29), so we can just ignore them.) Fortunately, many of the diagrams are simply related to each other. Crossing symmetry reduces the number of distinct diagrams to only six,

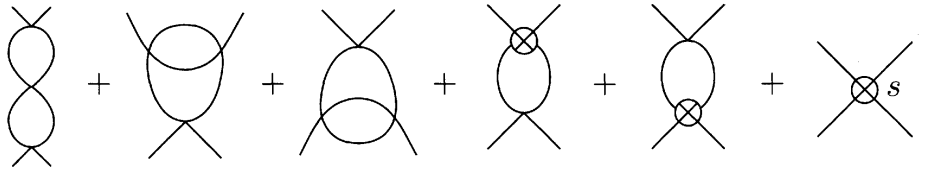

(10.51)

where the last diagram denotes only the s-channel piece of the second-order vertex counterterm. If this sum of diagrams is finite, then simply replacing s with t or u gives a finite result for the remaining diagrams.

The value of the last diagram in (10.51) is just a constant, which we can freely adjust to absorb any divergent terms that are independent of the external momenta. Our goal, therefore, is to show that all momentum-dependent divergent terms cancel among the remaining five diagrams.

The fourth and fifth diagrams in (10.51) involve the one-loop vertex counterterm, which we computed in Eq. (10.24). Let us briefly recall that computation. We defined $iV(p^2)$ as the fundamental loop integral,

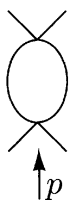

$$= (-i\lambda)^2 \cdot iV(p^2) = (-i\lambda)^2 \left[-\frac{i}{2} \frac{\Gamma(2-\frac{d}{2})}{(4\pi)^{d/2}} \int_0^1 dx \frac{1}{\left[m^2 - x(1-x)p^2\right]^{2-d/2}} \right]. \tag{10.52}$$

[‡]N. N. Bogoliubov and O. S. Parasiuk, *Acta Math.* **97**, 227 (1957); K. Hepp, *Comm. Math. Phys.* **2**, 301 (1966); W. Zimmermann, in Deser, et. al. (1970).

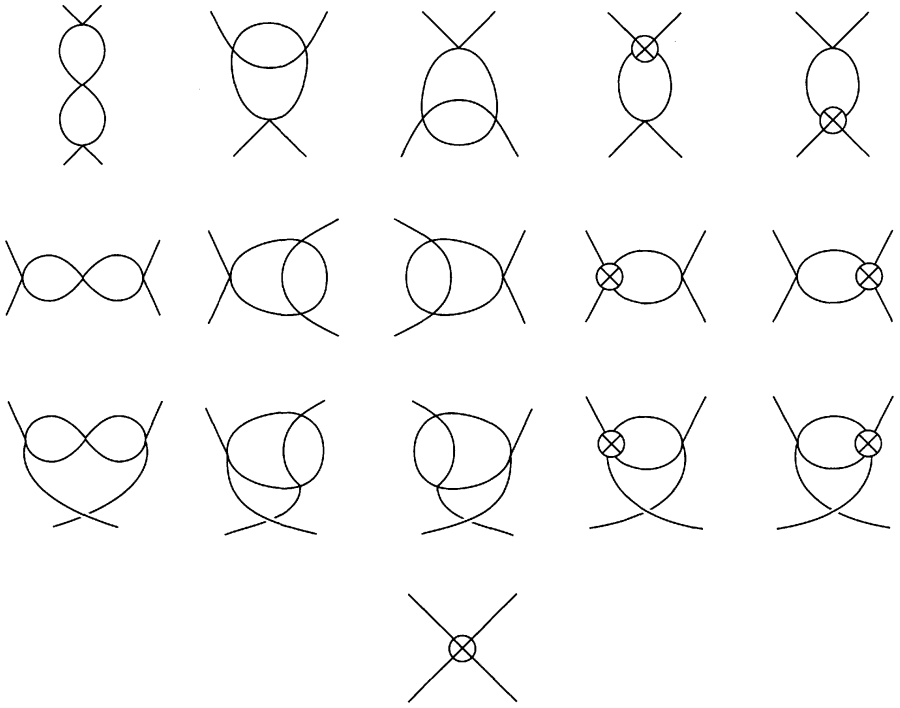

Figure 10.5. The two-loop contributions to the four-point function in ϕ^4 theory. Note that the diagrams in the first three lines are related to each other by crossing, being in the s-, t-, and u-channels, respectively. The last two diagrams in each of these lines involve the $\mathcal{O}(\lambda^2)$ vertex counterterm, while the final diagram is the $\mathcal{O}(\lambda^3)$ contribution to the vertex counterterm.

The counterterm, according to the renormalization condition (10.19), had to cancel the three one-loop diagrams (one for each channel) at threshold ($s = 4m^2$, $t = u = 0$); thus we found

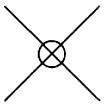

$$= -i\delta_\lambda = (-i\lambda)^2\big[-iV(4m^2) - 2iV(0)\big].$$

For our present purposes it will be convenient to separate the two terms of this expression. Let us therefore define

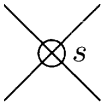

$$= (-i\lambda)^2 \cdot -iV(4m^2);$$

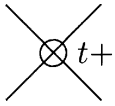

$$= (-i\lambda)^2 \cdot -2iV(0).$$

We can now divide the first five diagrams in (10.51) into three groups, as

follows:

Group I:

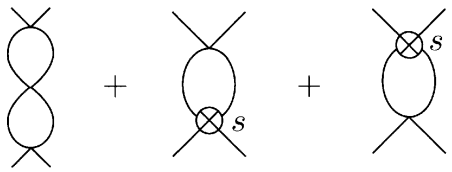

Group II:

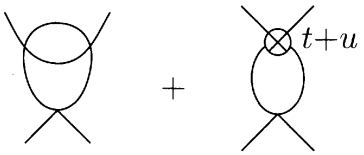

Group III:

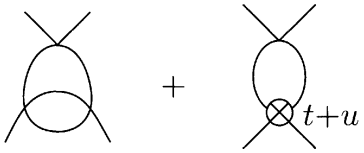

We will find that all divergent terms that depend on momentum cancel separately within each group. Since Groups II and III are related by a simple interchange of initial and final momenta, it suffices to demonstrate this cancellation for Groups I and II.

Group I is actually quite easy, since each diagram factors into a product of objects we have already computed. Referring to Eq. (10.52), we have

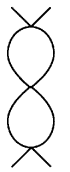

$$= (-i\lambda)^3 \cdot \left[iV(p^2)\right]^2;$$

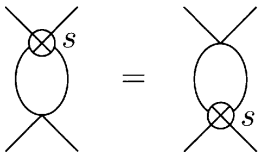

$$= (-i\lambda)^3 \cdot iV(p^2) \cdot -iV(4m^2).$$

The sum of all three diagrams is therefore

$$\begin{aligned}(-i\lambda)^3 &\Big(\left[iV(p^2)\right]^2 - 2iV(p^2)iV(4m^2)\Big) \\ &= (-i\lambda)^3\Big(-\left[V(p^2) - V(4m^2)\right]^2 + \left[V(4m^2)\right]^2\Big).\end{aligned} \tag{10.53}$$

But the difference $V(p^2)-V(4m^2)$ is finite, as was required for the cancellation of divergences in the one-loop calculation:

$$V(p^2) - V(4m^2) = \frac{1}{32\pi^2}\int_0^1 dx\, \log\left(\frac{m^2 - x(1-x)p^2}{m^2 - x(1-x)4m^2}\right).$$

The only remaining divergence is in the term $[V(4m^2)]^2$, which is independent of momentum and can therefore be absorbed into the second-order counterterm in (10.51).

Two general properties of result (10.53) are worth noting. First, the divergent piece (and hence the $\mathcal{O}(\lambda^3)$ vertex counterterm) is proportional to

$$\left[V(4m^2)\right]^2 \propto \left[\Gamma(2-\tfrac{d}{2})\right]^2 \underset{d\to 4}{\longrightarrow} \left(\frac{2}{\epsilon}\right)^2 \qquad \text{for } d = 4-\epsilon.$$

This is a double pole, in contrast to the simple pole we found for the one-loop counterterm. Higher-loop diagrams will similarly have higher-order poles, but in all cases the divergent terms are momentum-independent constants. Second, consider the large-momentum limit,

$$V(p^2) - V(4m^2) \underset{p^2\to\infty}{\sim} \log\frac{p^2}{m^2}.$$

The two-loop vertex is proportional to $\log^2(p^2/m^2)$. A diagram of this structure with n loops will have the form

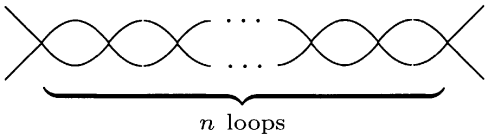

$$\sim \lambda^{n+1}\left(\log\frac{p^2}{m^2}\right)^n.$$

This asymptotic behavior is actually a generic property of multiloop diagrams, which we will explore in more detail in Chapter 12.

Now consider the more difficult diagram, from Group II:

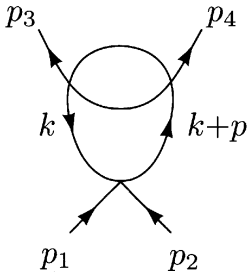

$$= (-i\lambda)^3 \int \frac{d^dk}{(2\pi)^d}\,\frac{i}{k^2-m^2}\,\frac{i}{(k+p)^2-m^2}\,iV\big((k+p_3)^2\big). \tag{10.54}$$

In evaluating this diagram, we will combine denominators in the manner that makes it most straightforward to extract the divergent terms, at the price of complicating the evaluation of the finite parts. Another approach to the calculation of this diagram is discussed in Problem 10.4.

To begin the evaluation of (10.54), combine the pair of denominators shown explicitly, and substitute expression (10.52) for $V(p^2)$. This gives the expression

$$-\frac{\lambda^3}{2}\frac{\Gamma(2-\frac{d}{2})}{(4\pi)^{d/2}}\int_0^1 dx\int_0^1 dy\int\frac{d^dk}{(2\pi)^d}\,\frac{1}{\left[k^2+2yk\cdot p+yp^2-m^2\right]^2}$$
$$\times\,\frac{1}{\left[m^2-x(1-x)(k+p_3)^2\right]^{2-\frac{d}{2}}}. \tag{10.55}$$

It is possible to combine this pair of denominators by using the identity

$$\frac{1}{A^\alpha B^\beta} = \int_0^1 dw \, \frac{w^{\alpha-1}(1-w)^{\beta-1}}{\big[wA+(1-w)B\big]^{\alpha+\beta}} \frac{\Gamma(\alpha+\beta)}{\Gamma(\alpha)\Gamma(\beta)}. \tag{10.56}$$

This is a special case of the formula quoted in Section 6.3, Eq. (6.42). To prove it, change variables in the integral:

$$z \equiv \frac{wA}{wA+(1-w)B}, \quad (1-z) = \frac{(1-w)B}{wA+(1-w)B}, \quad dz = \frac{AB\,dw}{\big[wA+(1-w)B\big]^2},$$

so that

$$\int_0^1 dw \, \frac{w^{\alpha-1}(1-w)^{\beta-1}}{\big[wA+(1-w)B\big]^{\alpha+\beta}} = \frac{1}{A^\alpha B^\beta} \int_0^1 dz \, z^{\alpha-1}(1-z)^{\beta-1} = \frac{1}{A^\alpha B^\beta} B(\alpha,\beta),$$

where $B(\alpha,\beta)$ is the beta function, Eq. (7.82). The more general identity (6.42) can be proved by induction.

Applying identity (10.56) to (10.55), we obtain

$$= -\frac{\lambda^3}{2} \frac{\Gamma(4-\frac{d}{2})}{(4\pi)^{d/2}} \int_0^1 dx \int_0^1 dy \int_0^1 dw \int \frac{d^dk}{(2\pi)^d} \times \frac{w^{1-\frac{d}{2}}(1-w)}{\big(w\big[m^2-x(1-x)(k+p_3)^2\big] + (1-w)\big[m^2-k^2-2yk\cdot p-yp^2\big]\big)^{4-\frac{d}{2}}}. \tag{10.57}$$

Completing the square in the denominator yields a polynomial of the form

$$-\big[(1-w)+wx(1-x)\big]\ell^2 - P^2 + m^2, \tag{10.58}$$

where ℓ is a shifted momentum variable and P^2 is a rather complicated function of p, p_3, and the various Feynman parameters. It will only be important for this analysis that, as $w \to 0$,

$$P^2(w) = y(1-y)p^2 + \mathcal{O}(w), \tag{10.59}$$

and this can be seen easily from (10.57). Changing variables to ℓ, Wick-rotating, and performing the integral, we eventually obtain

$$= -\frac{i\lambda^3}{2(4\pi)^d} \int_0^1 dx \int_0^1 dy \int_0^1 dw \, \frac{w^{1-\frac{d}{2}}(1-w)}{\big[1-w+wx(1-x)\big]^{d/2}} \frac{\Gamma(4-d)}{(m^2-P^2)^{4-d}}. \tag{10.60}$$

This expression has one obvious pole as $d \to 4$, coming from the gamma function. However, it also has a less obvious pole, coming from the zero end

of the w integral. Let us write (10.60) as

$$\int_0^1 dw\; w^{1-\frac{d}{2}}\, f(w),$$

where $f(w)$ incorporates all the factors not displayed explicitly. To isolate the pole at $w = 0$, we can add and subtract $f(0)$:

$$\int_0^1 dw\; w^{1-\frac{d}{2}}\, f(w) = \int_0^1 dw\, w^{1-\frac{d}{2}}\, f(0) + \int_0^1 dw\, w^{1-\frac{d}{2}}\, \big[f(w) - f(0)\big]. \quad (10.61)$$

The second piece is

$$-\frac{i\lambda^3\Gamma(4-d)}{2(4\pi)^d} \int_0^1 dx \int_0^1 dy \int_0^1 dw\; w^{1-\frac{d}{2}} \times \left(\frac{(1-w)}{\big[1-w+wx(1-x)\big]^{d/2}} \frac{1}{\big[m^2 - P^2(w)\big]^{4-d}} - \frac{1}{\big[m^2 - P^2(0)\big]^{4-d}} \right).$$

This term has only a simple pole as $d \to 4$; the residue of the pole is a momentum-independent constant, obtained by setting $d = 4$ everywhere except in $\Gamma(4-d)$. We can therefore absorb this divergence into the $\mathcal{O}(\lambda^3)$ vertex counterterm. (The finite part of this expression has a very complicated dependence on momentum, but we do not need to work this out to complete our argument.)

We are left with only the first term of (10.61). This expression contains only $P^2(0)$, which is given by (10.59). The w integral in this term is straightforward, and the x integral is trivial. With $\epsilon = 4-d$, our remaining expression is

$$-\frac{i\lambda^3}{2(4\pi)^d}\left(\frac{2}{\epsilon}\right) \int_0^1 dy\, \frac{\Gamma(\epsilon)}{\big[m^2 - y(1-y)p^2\big]^{\epsilon}}$$

$$\xrightarrow[d\to 4]{} -\frac{i\lambda^3}{2(4\pi)^4}\left(\frac{2}{\epsilon}\right) \int_0^1 dy \left(\frac{1}{\epsilon} - \gamma + \log(4\pi) - \log\big[m^2 - y(1-y)p^2\big] \right), \quad (10.62)$$

where we have kept only the divergent terms in the second line. The logarithm, multiplied by the pole $2/\epsilon$, is the nonlocal divergence that we worried about in Section 10.4.

Fortunately, we must still add to this the "$t+u$" counterterm diagram of Group II. The computation of that diagram is by now a straightforward

process:

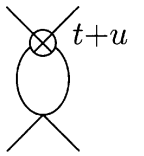

$$= (-i\lambda)^3 \cdot -2iV(0) \cdot iV(p^2)$$

$$= \frac{i\lambda^3}{2(4\pi)^d} \int_0^1 dy \, \frac{\Gamma(2-\frac{d}{2})}{\left[m^2\right]^{2-d/2}} \frac{\Gamma(2-\frac{d}{2})}{\left[m^2 - y(1-y)p^2\right]^{2-d/2}}$$

$$\xrightarrow[d\to 4]{} \frac{i\lambda^3}{2(4\pi)^4} \int_0^1 dy \left(\frac{2}{\epsilon} - \gamma + \log(4\pi) - \log m^2\right)$$

$$\times \left(\frac{2}{\epsilon} - \gamma + \log(4\pi) - \log\left[m^2 - y(1-y)p^2\right]\right). \quad (10.63)$$

(Again we have dropped finite terms from the last line.) This expression also contains a nonlocal divergence, given by the first pole times the second logarithm. It exactly cancels the nonlocal divergence in (10.62). The remaining terms are all either finite, or divergent but independent of momentum. This completes the proof that the two-loop contribution to the four-point function is finite.

The two features of the Group I diagrams appear here in Group II as well. The divergent pieces of (10.62) and (10.63) contain double poles that do not cancel, so we again find that the second-order vertex counterterm must contain a double pole. The finite pieces of (10.62) and (10.63) contain double logarithms, so we again find that the two-loop amplitude behaves as $\lambda^3 \log^2 p^2$ as $p \to \infty$.

Problems

10.1 One-loop structure of QED. In Section 10.1 we argued from general principles that the photon one-point and three-point functions vanish, while the four-point function is finite.

(a) Verify directly that the one-loop diagram contributing to the one-point function vanishes. There are two Feynman diagrams contributing to the three-point function at one-loop order. Show that these cancel. Show that the diagrams contributing to any n-point photon amplitude, for n odd, cancel in pairs.

(b) The photon four-point amplitude is a sum of six diagrams. Show explicitly that the potential logarithmic divergences of these diagrams cancel.

10.2 Renormalization of Yukawa theory. Consider the pseudoscalar Yukawa Lagrangian,

$$\mathcal{L} = \tfrac{1}{2}(\partial_\mu \phi)^2 - \tfrac{1}{2}m^2\phi^2 + \bar{\psi}(i\partial\!\!\!/ - M)\psi - ig\bar{\psi}\gamma^5\psi\phi,$$

where ϕ is a real scalar field and ψ is a Dirac fermion. Notice that this Lagrangian is invariant under the parity transformation $\psi(t, \mathbf{x}) \to \gamma^0\psi(t, -\mathbf{x})$, $\phi(t, \mathbf{x}) \to -\phi(t, -\mathbf{x})$,

in which the field ϕ carries odd parity.

(a) Determine the superficially divergent amplitudes and work out the Feynman rules for renormalized perturbation theory for this Lagrangian. Include all necessary counterterm vertices. Show that the theory contains a superficially divergent 4ϕ amplitude. This means that the theory cannot be renormalized unless one includes a scalar self-interaction,

$$\delta\mathcal{L} = \frac{\lambda}{4!}\phi^4,$$

and a counterterm of the same form. It is of course possible to set the renormalized value of this coupling to zero, but that is not a natural choice, since the counterterm will still be nonzero. Are any further interactions required?

(b) Compute the divergent part (the pole as $d \to 4$) of each counterterm, to the one-loop order of perturbation theory, implementing a sufficient set of renormalization conditions. You need not worry about finite parts of the counterterms. Since the divergent parts must have a fixed dependence on the external momenta, you can simplify this calculation by choosing the momenta in the simplest possible way.

10.3 Field-strength renormalization in ϕ^4 theory. The two-loop contribution to the propagator in ϕ^4 theory involves the three diagrams shown in (10.31). Compute the first of these diagrams in the limit of zero mass for the scalar field, using dimensional regularization. Show that, near $d = 4$, this diagram takes the form:

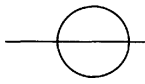

$$= -ip^2 \cdot \frac{\lambda^2}{12(4\pi)^4}\left[-\frac{1}{\epsilon} + \log p^2 + \cdots\right],$$

with $\epsilon = 4 - d$. The coefficient in this equation involves a Feynman parameter integral that can be evaluated by setting $d = 4$. Verify that the second diagram in (10.31) vanishes near $d = 4$. Thus the first diagram should contain a pole only at $\epsilon = 0$, which can be canceled by a field-strength renormalization counterterm.

10.4 Asymptotic behavior of diagrams in ϕ^4 theory. Compute the leading terms in the S-matrix element for boson-boson scattering in ϕ^4 theory in the limit $s \to \infty$, t fixed. Ignore all masses on internal lines, and keep external masses nonzero only as infrared regulators where these are needed. Show that

$$i\mathcal{M}(s,t) \sim -i\lambda - i\frac{\lambda^2}{(4\pi)^2}\log s - i\frac{5\lambda^3}{2(4\pi)^4}\log^2 s + \cdots.$$

Notice that ignoring the internal masses allows some pleasing simplifications of the Feynman parameter integrals.